Accepted Manuscript

Carbon sequestration via enhanced weathering of peridotites and basalts in seawater

Ioannis Rigopoulos, Anna L. Harrison, Andreas Delimitis, Ioannis Ioannou, Angelos M. Efstathiou, Theodora Kyratsi, Eric H. Oelkers

PII: S0883-2927(17)30339-6

DOI: 10.1016/j.apgeochem.2017.11.001

Reference: AG 3983

To appear in: *Applied Geochemistry*

Received Date: 5 September 2017

Revised Date: 30 October 2017

Accepted Date: 2 November 2017

Please cite this article as: Rigopoulos, I., Harrison, A.L., Delimitis, A., Ioannou, I., Efstathiou, A.M., Kyratsi, T., Oelkers, E.H., Carbon sequestration via enhanced weathering of peridotites and basalts in seawater, *Applied Geochemistry* (2017), doi: 10.1016/j.apgeochem.2017.11.001.

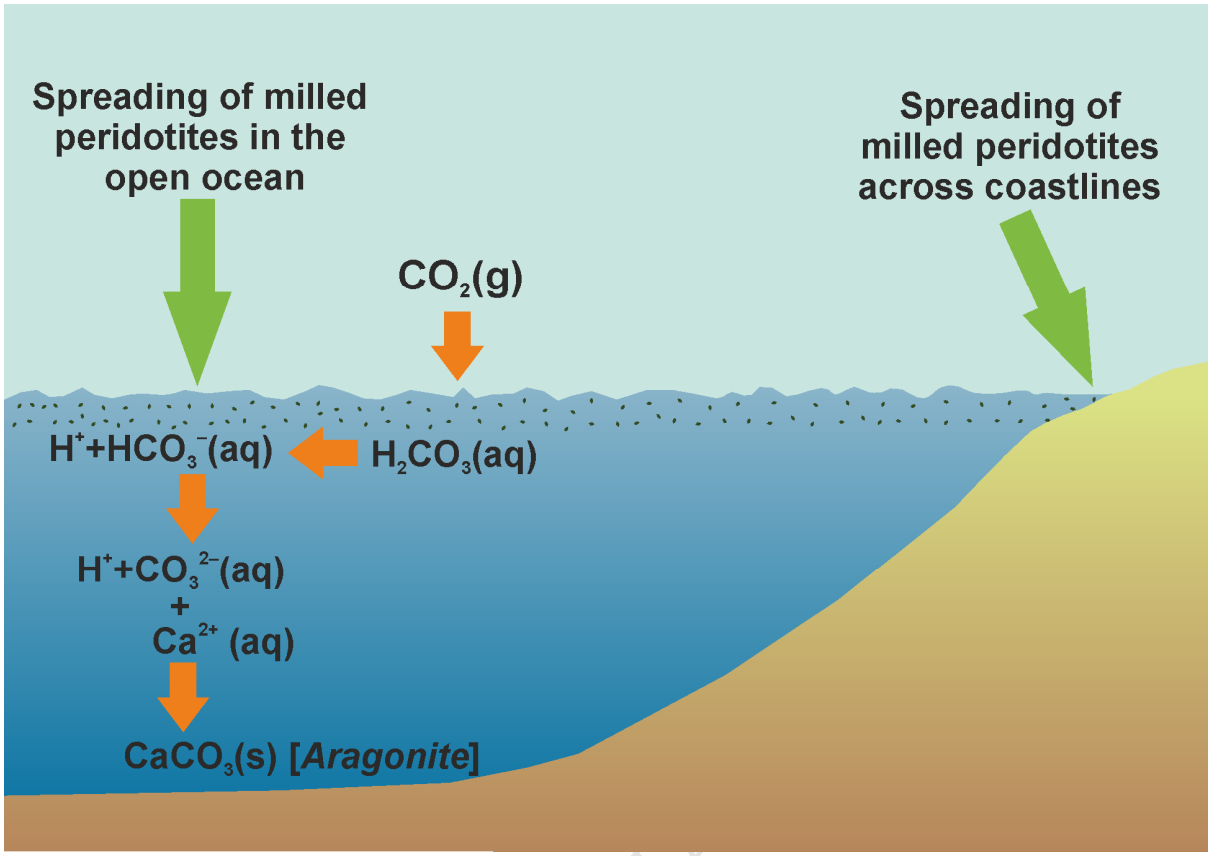

Carbon sequestration via enhanced weathering of peridotites and basalts in seawater

Ioannis Rigopoulos [a], Anna L. Harrison [b,c], Andreas Delimitis [d], Ioannis Ioannou [e], Angelos M. Efstathiou [f], Theodora Kyratsi [a], Eric H. Oelkers [b,c,g,*]

[a] *Department of Mechanical and Manufacturing Engineering, University of Cyprus, 1678 Nicosia, Cyprus*

[b] *Geoscience and Environment Toulouse (GET), CNRS, UMR 5563, Observatoire Midi-Pyrénées, 14 Avenue Edouard Belin, 31400 Toulouse, France*

[c] *Department of Earth Sciences, University College London, Gower Street, London WC1E 6DT, United Kingdom*

[d] *Chemical Process & Energy Resources Institute (CPERI), Centre for Research & Technology Hellas (CERTH), 6th km Charilaou – Thermis Road, GR-57001 Thermi, Thessaloniki, Greece*

[e] *Department of Civil and Environmental Engineering, University of Cyprus, 1678 Nicosia, Cyprus*

[f] *Department of Chemistry, Heterogeneous Catalysis Lab, University of Cyprus, 1678 Nicosia, Cyprus*

[g] *Institute of Earth Sciences, University of Iceland, Sturlugata 7, 101 Reykjavik, Iceland*

Corresponding Author

* E-mail: E. H. Oelkers: oelkers@get.omp.eu

E-mail addresses:

I. Rigopoulos: rigopoulos.ioannis@ucy.ac.cy

A. L. Harrison: anna.harrison@get.omp.eu

A. Delimitis: andel@cperi.certh.gr

I. Ioannou: ioannis@ucy.ac.cy

A. M. Efstathiou: efstath@ucy.ac.cy

T. Kyratsi: kyratsi@ucy.ac.cy

Abstract

Enhanced weathering of mafic and ultramafic rocks has been suggested as a carbon sequestration strategy for the mitigation of climate change. This study was designed to assess the potential drawdown of CO_2 directly from the atmosphere by the enhanced weathering of peridotites and basalts in seawater. Pulverized, and ball milled dunite, harzburgite and olivine basalt were reacted in artificial seawater in batch reactor systems open to the atmosphere for two months. The results demonstrate that the ball-milled dunite and harzburgite changed dramatically the chemical composition of the seawater within a few hours, inducing CO_2 drawdown directly from the atmosphere and ultimately the precipitation of aragonite. In contrast, pulverized but unmilled rocks, and the ball-milled basalt, did not yield any significant changes in seawater composition during the two-month experiments. As much as 10 weight percent aragonite was precipitated during the experiment containing the finest-grained dunite. These results demonstrate that ball milling can substantially enhance the weathering rate of peridotites in marine environments, promoting the permanent storage of CO_2 as environmentally benign carbonate minerals through enhanced weathering. The precipitation of Mg-silicate clay minerals, however, could reduce the efficiency of this carbon sequestration approach over longer timescales.

Keywords: Enhanced weathering; Basalts; Peridotites; Carbon capture and storage (CCS); Mineral carbonation; Clay minerals

1. Introduction

Human activities over the past century, particularly fossil fuel consumption, have caused a dramatic increase of CO_2 concentration in the atmosphere (e.g. IPCC, 2007; Oelkers and Cole, 2008). This anthropogenic impact on the global carbon cycle is considered to be the main reason for the observed climate change over the past decades (IPCC, 2005; Solomon et al., 2009). Global climate change has been linked to various other phenomena, including hurricanes, droughts, floods, glacier retreat, and rising sea levels (Emanuel, 2005; Rignot, 1998; Schiermeier, 2011; Trenberth et al., 2014). As such, large efforts have been made to develop effective carbon capture and storage (CCS) methods that remove CO_2 from the atmosphere (e.g. Gerdemann et al., 2007; Gislason and Oelkers, 2014; Lackner et al., 1995; Matter and Kelemen, 2009; Matter et al., 2016; Michael et al., 2010; Oelkers et al, 2008; Power et al., 2013, 2016; Wilson et al., 2014).

Chemical weathering is a slow process that controls atmospheric CO_2 concentrations over geological time scales. A number of scientists have proposed accelerating chemical weathering to counter global climate change (Griffioen, 2017; Hartmann et al., 2013; Köhler et al., 2010, 2013; Lackner, 2003; Montserrat et al., 2017; Schuiling and De Boer, 2011; Schuiling and Krijgsman, 2006; Seifritz, 1990; Taylor et al., 2016). The goal of enhanced weathering is to hasten silicate mineral weathering rates to accelerate the removal of CO_2 from the atmosphere as dissolved inorganic carbon and/or as carbonate minerals. Because of their relatively rapid dissolution rates, enhanced weathering has focused on mafic and ultramafic rocks (Hartmann et al., 2013; Hauk et al., 2016; Moosdorf et al., 2014; Renforth, 2012; Taylor et al., 2016). Experimentally measured dissolution rates of Wolff-Boenisch et al. (2011) suggest that ground mafic and ultramafic rocks could lead to the efficient carbon dioxide mineralisation in seawater. One method to accelerate weathering rates is to increase rock surface area by crushing, grinding,

and/or milling (Renforth, 2012). The grinding process can increase specific dissolution rates through "mechano-chemical activation" (Balaz et al., 2008; Gerdemann et al., 2007). Past studies have also demonstrated that milling can dramatically increase the reactivity of Mg-silicates by reducing particle size to > 1 μm (e.g. Haug et al., 2010; Rigopoulos et al., 2015, 2016a, 2016b; Turianicová et al., 2013). The effect of mechanical activation on the carbon sequestration efficiency of ultramafic rocks/mine waste materials has been reported by Li and Hitch (2016a, b; 2017a, b). Schuiling and De Boer (2011) suggested that even relatively large olivine grains might completely dissolve within 1-2 years in high-energy shallow marine environments. In contrast, Hangx and Spiers (2009) estimated that olivine particles of 10 μm need approximately 23 years to completely dissolve, although Renforth (2012) suggested this estimate was 30% too high. Moreover, Köhler et al. (2013) suggested that only olivine particles with a grain size on the order of 1 μm would sink slowly enough to enable their nearly complete dissolution.

The goal of this study is to assess the potential for the enhanced weathering of peridotites and basalts in seawater to facilitate the drawdown of atmospheric CO_2. Towards this goal, we reacted two ultramafic rocks and one mafic rock in artificial seawater in open system reactors. The rock samples were subjected to different degrees of ball milling to produce powders of distinct sizes and surface area. The purpose of this communication is to report the results of this experimental study and to use these results to illuminate the potential role of enhanced ultramafic and mafic rock weathering in seawater as a viable CCS technique.

2. Materials and methods

2.1. Sample selection, preparation and characterization

The rocks used in this study were collected from the Troodos ophiolite complex; this complex was formed in a supra-subduction zone environment around 92-90 Ma ago (Mukasa and Ludden, 1987; Robertson, 2002; Robinson and Malpas, 1990). In the present study, two peridotites were collected from the Troodos mantle section: one dunite and one harzburgite, both of which are partially serpentinized. Additionally, an olivine basalt was collected from the "Upper" Pillow Lava unit of the Troodos ophiolite. The mineralogical and textural characteristics of these rock samples were determined by petrographic analysis of representative thin sections using a polarizing microscope (Figs. S1-S3 in the electronic supplement). Whole-rock chemical analyses were also performed using a combination of lithium metaborate/tetraborate fusion inductively coupled plasma (ICP), inductively coupled plasma mass spectroscopy (ICP-MS) and instrumental neutron activation analysis (INAA) techniques (Tables S1 and S2 in the electronic supplement). Fine-grained samples were initially prepared using a stainless steel pulverizer and then sieved to obtain the 104-150 μm size fraction. This fraction was cleaned ultrasonically ten times in ethanol to remove fine particles; and then dried overnight at 50 ºC. The specific surface area of this fraction for each rock sample was measured by the BET method (Table 1). A portion of this size fraction was used directly in the experiments, while the remainder was ball-milled to further reduce its grain size as described in section 2.2. The non-ball-milled size fraction is henceforth referred to as "unmilled". Additional enhanced weathering experiments were performed using selected ball-milled samples.

2.2. Ball milling

Ball milling (BM) was performed using a Fritsch Pulverisette 6 planetary mono mill. The optimum milling conditions for basaltic and ultramafic rocks were applied, based on the results

of previous studies (Rigopoulos et al., 2015, 2016a). The peridotites and basalt were wet-milled in an 80 mL tungsten carbide bowl using ethanol as process control agent (PCA). The selection of this PCA is based on recent experimental results (Rigopoulos et al., 2015, 2016a), which demonstrated that the use of ethanol during ball milling promotes the formation of smaller, more uniform and rounded particles compared to H_2O. In our experiments, the ball-to-powder mass ratio was 20:1 w/w, the fluid-to-powder mass ratio was 1:2 and the rotation speed was 300 rpm. The process was performed using 30 tungsten carbide balls with a 10 mm diameter. Tungsten carbide bowl and balls were used to avoid possible contamination due to the hardness of ultramafic and mafic rocks. Ball milling was automatically interrupted every 5 min for 5 min to avoid sample heating. This periodic interruption avoids phase transformations and reduces the evaporation of the PCA. After milling was complete, the recovered rock powders were dried overnight at room temperature. The enhanced weathering experiments described below were performed using the ball-milled samples with the highest BET specific surface area (see Fig. 1). For the dunite, an additional ball-milled sample was used to clarify the role of ball milling duration on chemical weathering rates. The correlations between the specific surface area and the ball milling duration for each rock type are shown in Fig. 1. Initially, an increase of milling time yields higher specific surface areas; however, these positive trends may become negative with additional milling (Fig. 1). This behavior can be attributed to particle agglomeration occurring after a few hours of milling (Rigopoulos et al., 2015, 2016a, 2016b). The milling conditions and specific surface areas of the studied rock materials are summarized in Table 1.

[Insert Fig. 1 approximately here]

2.3. Experimental design

Experiments were performed in 1000 mL polypropylene batch reactors at ambient temperature and pressure conditions (T: 23.5±1.5 ºC, P: 1 atm; Fig. 2). Initially, each reactor was loaded with 1.6 g of rock material and 800 mL of artificial seawater (rock/fluid ratio: 2 g/L). The artificial seawater was prepared based on the composition of Millero et al. (2006) (Table S3 in the electronic supplement). Artificial seawater was to used in this study to exclude any potential biological processes that would increase the complexity of the results. Prior to the experiments, laboratory air was bubbled through the artificial seawater solution for ~24 h to reach equilibrium with respect to atmospheric CO_2, as confirmed by dissolved inorganic carbon measurements of the initial solution. The reactors were continuously shaken using orbital shakers (KS 260 basic IKA®) with a rotational speed of 200 rpm to mimic wave action. The rock materials remained largely in suspension throughout the experiments due to the relatively low rock/fluid ratio. The goal was to mimic the coastal ocean, where the rock material would be in suspension due to the action of waves and currents. Each experiment lasted 2 months, and each reactor was open to the atmosphere during the experiments (Fig. 2). The sampling outlet of each reactor was loosely covered to prevent dust entry, but allowing gas exchange with the atmosphere. A total of 16 fluid samples (volume of each sample: ~8 mL) were collected from each experiment using filtered polypropylene syringes, at selected times. Consequently, ~16% of the reactive fluid was removed via sampling by the end of the experiment. As the solids largely remained in suspension during sampling, there was not a significant change in the rock/fluid ratio in the reactors. The fluid samples were subsequently filtered using 0.02 μm alumina based membrane filters. An aliquot was acidified to 2% HNO_3 prior Si, Mg and Ca concentration analysis, while the remainder was stored with no headspace for dissolved inorganic carbon (DIC) analysis. At the end of the

163 experiments, the solids were collected using vacuum filtration and dried for a few days at room
164 temperature.

165 *[Insert Fig. 2 approximately here]*

166 A total of eight experiments was performed: one control experiment containing only
167 artificial seawater, three experiments with unmilled rock materials, two experiments with ball-
168 milled dunite after distinct ball milling durations, one experiment with ball-milled harzburgite,
169 and one experiment with ball-milled olivine basalt (see Table 1 for further sample details).

170

171 *2.4. Fluid and solid sample analyses*

172 The reactive fluid pH was measured in the reactors using a Metrohm 913 pH-meter and a
173 Metrohm combined electrode (6.0234.1000). Before each use, the electrode was calibrated using
174 three NIST buffer solutions (pH 4.008, 6.865, and 9.180 at 25 ºC, Fluka). The concentrations of
175 total dissolved inorganic carbon (DIC) in all fluid samples were measured using a Shimadzu
176 TOC-V_{CSN} analyzer, in combination with an ASI-V automatic sampler. The dissolved Si, Mg
177 and Ca concentrations were determined on the acidified samples using inductively coupled
178 plasma atomic emission spectroscopy (ICP-AES). Mineral saturation states of the reactive fluids
179 were determined using measured pH, and DIC, Si, Mg, and Ca concentrations, together with
180 PHREEQC V3 and its llnl database (Parkhurst and Appelo, 2013). Detection limits and
181 uncertainties of these analyses are provided in section 4 of the electronic supplement.

182 The precipitation of carbonate minerals during the experiments was investigated by
183 measuring the total inorganic carbon in the solids before and after the experiments using a
184 Horiba EMIA-320V Carbon/Sulfur analyzer. Furthermore, the solids were characterized by
185 powder X-ray diffraction (PXRD), scanning electron microscopy (SEM) and energy dispersive

spectroscopy (EDS). In addition, conventional transmission electron microscopy (TEM), as well as high-resolution transmission electron microscopy (HRTEM) studies were performed (see electronic supplement for detailed methods).

3. Results and discussion

3.1. Fluid chemical compositions

The initial pH of the artificial seawater in equilibrium with atmospheric CO_2 was 8.06, within the pH range of natural seawater (Marion et al., 2011). Fig. 3 illustrates the evolution of pH during the 2-month experiments (see also Table S4 in the electronic supplement). The pH of the fluids containing the three different unmilled rock materials did not show any significant changes over time (Fig. 3a and b). In contrast, the ball-milled dunite and harzburgite induced a substantial increase of pH near the beginning of the experiments (Fig. 3a and b). This pH increase could be attributed to the dissolution of olivine and other Mg-silicate minerals (e.g. Casey and Westrich, 1992; Declercq et al., 2013; Hänchen et al., 2006; Johnson et al., 2014; Oelkers, 2001; Oelkers et al., 2015; Pokrovsky and Schott, 2000; Wang and Giammar, 2013). After 6 hours, the most milled dunite provoked the greatest pH increase, followed by the milled harzburgite and the less milled dunite. The pH then decreased over time in these experiments. This pH decrease occurred earlier in the experiment with the less milled dunite compared to that with the most milled dunite (Fig. 3a), indicating an impact of milling duration on the reactivity of ultramafic rocks in seawater. In addition, the earlier decrease of pH in the milled harzburgite experiment compared to that with the most milled dunite (Fig. 3a and b) could be attributed to the higher olivine content and lesser degree of serpentinization in the dunite (see Petrography in

208 the electronic supplement). In contrast, little change in fluid pH was documented for either the
209 milled or the unmilled basalt sample (Fig. 3b).

210 *[Insert Fig. 3 approximately here]*

211 The DIC concentrations of the fluids in the unmilled peridotites and basalt experiments did
212 not exhibit any significant variations over time (Fig. 4; Table S5 in the electronic supplement;
213 see also the calculated total alkalinity in Table S6). Note that the DIC values of the reactive
214 fluids in the unmilled sample experiments are close to the initial DIC concentration (~25 ppm)
215 (see Table S3 in the electronic supplement) throughout the experiments. In contrast, the fluid
216 samples collected from the milled dunite and harzburgite experiments first show a decrease in
217 DIC followed by an increase towards the initial DIC concentrations (Fig. 4a and b). The highest
218 DIC values for these experiments were attained from fluid samples collected after over 500 hours
219 of reaction. The initial decrease of DIC from the fluids collected from the most milled peridotite
220 experiments suggests that precipitation of carbonate minerals began within the first few hours.
221 The fluids collected from the milled harzburgite and the less milled dunite experiments attained
222 their lowest DIC values after 24 h (Fig. 4a and b). Note that the most milled dunite experiment
223 attained a substantially lower DIC value than any other experiment (Fig. 4a and b), suggesting
224 that this ultrafine sample facilitated the greatest precipitation of carbonate minerals. On the other
225 hand, the DIC concentrations in the reactive fluids collected from the unmilled and milled
226 olivine basalt experiments do not show any noticeable temporal evolution, with similar DIC
227 concentrations as the control throughout the experiment (Fig. 4b). Such results are coherent with
228 the observation that the milled peridotites caused a sharp increase of seawater pH within the first
229 few hours of the experiments, whereas the basalt did not (see Fig. 3).

230 *[Insert Fig. 4 approximately here]*

The temporal evolution of Si, Mg and Ca concentrations in the reactive fluids can be seen in Fig. 5, and the results are summarized in Tables S7 and S8 in the electronic supplement. The Si trends indicate a large difference between the dissolution rate of the unmilled and ball-milled rocks. This observation is consistent with Hangx and Spiers (2009), who concluded that the dissolution rate of olivine is markedly enhanced when its grain size is <10 μm. Meysman and Montserrat 2017) argued that the dissolution rates could be further enhanced under natural conditions through various forms of biological activity in marine sediments, despite the fact that a number of studies suggest that microbes tend to slow rather than accelerate Mg-silicate dissolution reactions (Shirokova et al., 2012; Garcia et al., 2013; Oelkers et al., 2015). The milled basalt experiment exhibited lower reactive fluid Si concentrations compared to the milled ultramafic rocks, indicating its lower reactivity. The aforementioned difference between peridotites and basalts is in agreement with their corresponding pH and DIC trends (see Figs. 3 and 4). Nevertheless, there is a significant difference in the reactive fluid Si concentrations between the unmilled and ball-milled basalt experiments (Fig. 5a), implying that ball milling enhanced the dissolution rates of this sample. However, this is not accompanied by a noticeable increase of pH (Fig. 3b), suggesting that the increased Si concentrations in the milled basalt experiment are not only attributed to the enhanced dissolution of olivine, but also of other silicate minerals (e.g. augite, chlorite; see Petrography in the electronic supplement), which may limit the pH increase. As illustrated in Fig. 5a, the reactive fluids become more concentrated in Si over time; however, the fluids in the experiments with the most milled dunite and the milled harzburgite show a sharp decrease of Si during the first 73 and 50 hours, respectively. This decrease is most pronounced for the most milled dunite. In both experiments, a second stage of

253 decrease can be observed later. This suggests that Si is being removed from solution due to
254 precipitation of Si-bearing secondary phases.

255 The Mg concentrations do not exhibit clear temporal trends, presumably due to the high
256 initial Mg concentration of the artificial seawater (see Table S3 in the electronic supplement).
257 Nevertheless, a moderate increase in Mg concentrations can be observed over time, primarily in
258 the milled sample experiments (Fig. 5b). In addition, a decrease in Mg concentration is observed
259 in the most milled dunite and milled harzburgite experiments after 819 and 437 hours,
260 respectively. These reduced Mg concentrations are coherent with the reduced Si concentrations
261 after 819 and 437 hours in the same experiments (see Fig. 5a), suggesting the precipitation of a
262 Mg-silicate phase.

263 The reactive fluid Ca concentrations collected from the experiments with the unmilled
264 rocks and the milled basalt remained relatively unchanged during the 2-month experiments (Fig.
265 5c). In contrast, the reactive fluids from the experiments with the milled dunite and harzburgite
266 show an appreciable Ca concentration decrease with time. This decrease is coincident with the
267 initial negative DIC trends of these fluids (see Fig. 4). These observations suggest that the milled
268 ultramafic rocks promote the reaction between the Ca^{2+} pre-existing in the artificial seawater and
269 the dissolved inorganic carbon, leading to $CaCO_3$ precipitation. This Ca concentration decrease
270 is most pronounced in the most milled dunite experiment (Fig. 5c).

271 *[Insert Fig. 5 approximately here]*

272 According to mineral saturation state calculations (Tables S9-S15 in the electronic
273 supplement), aragonite and calcite were supersaturated in all reactive fluid samples, consistent
274 with natural seawater. However, the saturation index values of these minerals were not
275 substantially elevated. Notably, the temporal pH, DIC and aqueous Ca trends (see Figs. 3, 4 and

5c) of the milled dunite and harzburgite experiments are consistent with $CaCO_3$ precipitation (Fig. 6). In addition, speciation calculations suggest that magnesite [$MgCO_3$] was supersaturated during all experiments (Tables S9-S15 in the electronic supplement), though consistent with past studies (e.g. Saldi et al., 2009) it was not found to form during any experiment. Moreover, sepiolite, a Mg-silicate clay mineral, was supersaturated in the experiments with the milled samples, and especially in the experiments with the most milled dunite and milled harzburgite (Fig. 6f and i). Similarly, Okland et al. (2014) reported that sepiolite was supersaturated in the reactive fluids of low temperature dunite dissolution experiments, implying that its precipitation was thermodynamically possible.

[Insert Fig. 6 approximately here]

3.2. Solid compositions

The total inorganic carbon content of the solids before and after the experiments was measured. These results, as well as the calculated weight percent of $CaCO_3$ are listed in Table 2. The unmilled samples show only small changes in total inorganic carbon during the experiments. This is in agreement with Montserrat et al. (2017), who performed similar enhanced weathering experiments using forsteritic olivine. In contrast, the milled ultramafic rocks exhibit a large increase of total inorganic carbon during the experiments, with the most milled dunite having the highest amount of $CaCO_3$ (i.e., 10 wt%), consistent with observed fluid compositions (Table 2). This result clearly shows that carbonation increases notably with increasing milling time for ultramafic rocks. This is also consistent with the results acquired through CO_2 chemisorption followed by temperature-programmed desorption (CO_2-TPD) experiments in dunites (Rigopoulos et al., 2016a). The substantial reduction of particle size (see Fig. 7) and the

distortion of the mineral structure as evidenced by the XRD patterns shown in section 7 of the electronic supplement after ball milling is likely the reason for the enhanced carbonation rates. Note also that the absence of carbonate minerals in the ultramafic rocks before the experiments (see Table 2), excludes the idea of a seeded precipitation due to the availability of carbonate surface area (Renforth and Henderson, 2017). The presence of Mg-rich minerals, however, has been shown to enhance the nucleation of $CaCO_3$ from mildly supersaturated aqueous solutions (Stockmann et al., 2014). Although the formation of $CaCO_3$ in this system does fix securely CO_2 as a stable mineral phase, its formation in seawater releases protons thereby lowering the overall efficiency of enhanced weathering compared to just the addition of alkalinity. It seems likely that this process could be optimized by changing the mineral surface area to seawater ratio to alter the degree of supersaturation of secondary phase in the fluid.

The results obtained for the milled olivine basalt show that the content of total inorganic carbon increased only to a small extent during the experiment, consistent with the minor change of the reactive fluid composition of this experiment. Although milling led to an increased rate of Si release from the basaltic sample, its dissolution did not drive an increase in fluid pH, likely due to the dissolution of other silicate phases (e.g. augite or chlorite), rather than olivine. This observation is in agreement with the results reported by Taylor et al. (2016), who reported that the CO_2 consumption induced by terrestrial weathering of dunites and harzburgites is about twice that of basalts.

[Insert Fig. 7 approximately here]

Note that the measured total carbon contents of the recovered solids are in good agreement with corresponding $CaCO_3$ contents calculated from the temporal reactive fluid compositional evolutions (Fig. 8; Table 2). Furthermore, these fluid composition trends indicate that most

carbonate mineral precipitation occurred within the first hours of the experiments containing milled ultramafic rocks, while subsequently the rates slow dramatically (Fig. 8). The rapid precipitation of $CaCO_3$ in the most milled dunite and milled harzburgite experiments is also accompanied by a sharp decrease of the reactive fluid pH (Fig. 3). The abrupt reduction of $CaCO_3$ precipitation rates could be attributed to the rapid Ca^{2+} removal from solution during the first hours of the experiments, which decreases the saturation index of $CaCO_3$ phases towards equilibrium (see Fig. 6). Note also that the solids exhibited a rusty color after the experiments, suggesting that minor Fe-hydroxide precipitation could be an additional reason for the slower carbonation rates over time. Although the carbonate mineral precipitation almost stops near the beginning of the experiment with the less milled dunite (Fig. 8a), the most milled dunite experiment shows a continuous, albeit slow, increase of $CaCO_3$ over time (Fig. 8b), thus confirming the positive effect of milling duration on mineral carbonation. In addition, the fast $CaCO_3$ precipitation near the beginning of the experiments results in a reduced DIC concentration (Fig. 4), indicating that mineral carbonation rates may be limited by the supply rate of CO_2 from the atmosphere to the aqueous solution. This is consistent with observations of accelerated carbonation in mine tailings (Harrison et al., 2013; Wilson et al., 2010, 2014) and field-scale experimental basalt weathering (van Haren et al., 2017).

[Insert Fig. 8 approximately here]

XRD patterns of the rock materials were acquired before and after ball milling. Milling caused a substantial reduction in the intensity of all XRD peaks and led to the disappearance of some smaller peaks (Figs. S4-S6 in the electronic supplement). These observations suggest the structural disordering of the constituent silicate minerals, which is considered as one of the most important factors for enhancing carbonation reactions (Kleiv and Thornhill, 2006; Li and Hitch,

2016a; Munz et al., 2012; Rigopoulos et al., 2016b; Turianicová et al., 2013). The reduction in peak intensity due to ball milling is less evident in the milled basalt compared to the milled dunite obtained after the same milling duration (compare Figs. S4a, b and S6a, b in the electronic supplement); this is consistent with the substantially lower reactivity of the milled basalt compared to the milled peridotites. The distinct behavior of basalt could be attributed to the presence of an appreciable amount of chlorite (see Petrography in the electronic supplement), which is flexible and tends to absorb the applied stress (e.g. see Rigopoulos et al., 2013), thereby increasing the resistance of the rock material to mechanical deformation. Although the dunite and harzburgite contain serpentine, the mechanical behavior of which is similar to chlorite, its amount is smaller compared to that of chlorite in basalt.

In addition, XRD analyses were performed for each solid sample before and after the experiments. The results confirmed that the $CaCO_3$ in the milled ultramafic solids during the experiments was aragonite (Fig. S7 in the electronic supplement). Note that aragonite has a higher solubility compared to calcite and for a given pCO_2 it may sequester less carbon than calcite (Sun et al., 2015). Nevertheless, this is not expected to affect the carbon sequestration efficiency of the enhanced weathering approach described here, as aragonite is relatively stable over geologic time. The formation of aragonite in our experiments is consistent with previous observations of $CaCO_3$ precipitation from Mg-rich fluids; a Mg/Ca fluid concentration ratio greater than 2 favors aragonite precipitation (De Choudens-Sánchez and González, 2009; Morse et al., 1997, 2007; Sun et al., 2015). In our experiments, the Mg/Ca ratios of all reactive fluid samples range between 3.09 and 5.35 (see Tables S7 and S8 in the electronic supplement). The saturation index of aragonite was found to decrease to ~0.2 in the milled dunite and milled harzburgite experiments after ~400 h (Fig. 6a,d,g), coincident with the decrease of pH, recovery

of DIC concentrations towards the initial values, and reductions in the rate of Ca^{2+} removal from solution (Figs. 3, 4 and 5c). This suggests that the extent of carbonate precipitation was controlled by the aragonite saturation state; as the saturation index of aragonite declines towards equilibrium, precipitation rates slow to negligible values. Thus, although the short-term (hours to days) precipitation rates may be limited by the rate of CO_2 uptake into fluid, the longer-term (weeks to months) rates are limited by the rate of mineral dissolution to release cations and increase fluid pH.

Chemical mapping by SEM/EDS confirmed that Ca was abundant and fairly homogeneously distributed in the milled ultramafic solids recovered at the end of the experiments (Fig. S8 in the electronic supplement). However, it was not possible to obtain clear images of individual aragonite crystals using SEM, due to their small size. Consequently, TEM and HRTEM studies were also performed, which revealed that aragonite exists in the form of (i) up to 300 nm crystals (Fig. 9a), and (ii) nanocrystals with sizes in the range of 5-16 nm (Fig. 9b). The larger aragonite crystals are highly crystalline, as illustrated by HRTEM imaging (inset in Fig. 9a). EDS point analysis results confirmed that the newly formed aragonite is pure $CaCO_3$. The HRTEM images also show that the olivine in the ball-milled rock samples was structurally disordered (Fig. 9c); this disordering is likely responsible for the fast mineralization that took place near the beginning of the milled peridotite experiments. In addition, TEM/EDS observations revealed that a small amount of sepiolite [$Mg_4Si_6O_{15}(OH)_2 \cdot 6H_2O$] precipitated during the most milled peridotites experiments (Fig. 9d). The precipitation of this poorly crystalline secondary Mg-silicate (see the diffuse intensity rings of the selected area diffraction (SAD) pattern inset of Fig. 9d), is consistent with the decreasing Si concentration observed during the most milled dunite and milled harzburgite experiments (see Fig. 5a), as well as with

391 the calculated sepiolite saturation state (Fig. 6f,i). Although sepiolite remains supersaturated
392 throughout the experiments (Fig. 6f,i), its precipitation is followed by a recovery of Si
393 concentrations towards the initial values (Fig. 5a). This is coincident with the fast pH decrease
394 (Fig. 3), suggesting that the precipitation of this secondary mineral is favored in seawater with
395 high pH values. These results are also in agreement with previous studies, which report that
396 sepiolite is found in marine environments with olivine-rich ultramafic rocks (Bonatti et al.,
397 1983). Recently, Griffioen (2017) concluded that sepiolite precipitation is unfavourable for CO_2
398 storage during enhanced olivine weathering in marine environments, as its formation reduces
399 significantly the consumption of CO_2 per unit olivine. Although only a small amount of sepiolite
400 was precipitated during our experiments, its formation would reduce the efficiency of this carbon
401 sequestration approach by consuming protons and lowering pH, particularly over the longer term
402 as clay minerals have far slower precipitation rates than carbonate minerals.

403 *[Insert Fig. 9 approximately here]*

404

405 **4. Implications for carbon capture and storage**

406 One of the major challenges of enhanced weathering is the scale of mining and milling of
407 rock materials. Several studies focused on the total energy requirements of enhanced weathering
408 (Hangx and Spiers, 2009; Moosdorf et al., 2014). In general, CO_2 emissions and the associated
409 costs increase with decreasing grain size. According to Hangx and Spiers (2009), for final grain
410 sizes larger than ~40 μm, the CO_2 sequestration efficiency is reduced by less than 2%. However,
411 the CO_2 emissions resulting from mining, crushing and milling to achieve a final grain size on
412 the order of 10 μm, comprise between 5 and 11% of the total amount of sequestered CO_2. In
413 addition, Köhler et al. (2013) concluded that the energy consumption for milling to a 1 μm grain

size can reduce carbon sequestration efficiency by ~30%. Furthermore, the transportation of the rock material from the mine to the enhanced weathering site will further reduce the efficiency by 1.6-11.0 kg CO_2/100 km/tonne CO_2 sequestered or by 0.1-1% (Hangx and Spiers, 2009). This indicates that carbon sequestration via enhanced weathering in seawater would be more efficient by using rocks located near coastlines. As such, the high cost and CO_2 emissions related to the production and transportation of ultrafine rocks may limit the large-scale implementation of this enhanced weathering approach. The efficiency of this approach could be further reduced by the potential intense wear of the ball milling equipment (Haug et al., 2010). Additionally, the efficiency of comminution processes is very low (e.g., Radziszewski, 2013). All of these studies indicate that the mining, crushing, milling and transportation steps related to enhanced weathering must be optimised before its large-scale application.

Despite the energy required to produce ultrafine powders, our results suggest that the enhanced weathering of milled ultramafic rocks in seawater could facilitate CO_2 storage through mineralization. Note that mineral carbonation in our experiments occurred at ambient conditions. Although carbon storage via dissolved bicarbonates (i.e. increase of seawater alkalinity) may be more efficient as it requires less rock material per mole of CO_2 stored (e.g. Hangx and Spiers, 2009), mineral carbonation insures a long-term and more secure CO_2 storage. Once CO_2 is transformed into carbonate minerals, leakage risk is eliminated and any monitoring program can be reduced, potentially rendering this CCS approach more cost-effective. In addition, our experiments were not performed using pure olivine but partially serpentinized peridotites that, although less reactive compared to fresh ultramafic rocks, are readily available on the Earth's surface (e.g. see the peridotite distribution map in Matter and Kelemen, 2009). This potentially reduces the transport distances from the mine to the enhanced weathering site and therefore

facilitates the potential application of this approach on a global scale. Note also that the energy required to reduce the grain size of altered peridotites is substantially lower compared to that required for harder fresh ultramafic rocks. Furthermore, this enhanced weathering process removes carbon directly from the atmosphere, providing capture and storage in a single step.

The enhanced weathering of ultramafic rocks in seawater may also help avert ocean acidification, which has drastic consequences for marine ecosystems (Doney et al., 2009; Hoegh-Guldberg et al., 2007; Orr et al., 2005). Ocean acidification also entails a reduced saturation of surface seawater with respect to $CaCO_3$, threatening coral reefs with extinction (Caldeira and Wickett, 2003; Ricke et al., 2013). Here, we demonstrated that the distribution of milled peridotites in marine environments favors aragonite precipitation, thereby potentially helping to maintain the viability of coral reef ecosystems (see also Taylor et al., 2016). Enhanced weathering approaches may also affect marine life in unanticipated ways. The dissolution of olivine leads to an increase in dissolved Si. This process would alter marine biology because Si is the limiting nutrient for diatom growth over large sections of the oceans (Dugdale and Wilkerson, 1998; Ragueneau et al., 2006). Such a process could shift phytoplankton species composition towards diatoms, thus altering the biological carbon pumps (Köhler et al., 2013). Note that our experiments were performed in the absence of biological activity, which may influence, somewhat the rates and reactions paths of the studies reactions.

Note also that the geoengineering of the marine environment has been controversial. For example, in 2008 the United Nations Convention on Biological Diversity put a moratorium on all ocean fertilization activities apart from small coastal projects (Tollefson, 2008). Application of enhanced weathering on a global scale would require large amounts of ultramafic rocks (Hangx and Spiers, 2009; Taylor et al., 2016). Further efforts, therefore need to be made to assess the

environmental impacts of enhanced wreathing in marine environments towards the potential public acceptance of this approach.

5. Conclusions

This experimental study demonstrates that the "enhanced weathering" of ball-milled peridotites in seawater can induce the drawdown of CO_2 directly from the atmosphere. In contrast, the ball-milled basalt did not yield many significant changes in seawater composition due to its distinct mineralogy and higher resistance to mechanical deformation compared to peridotites. In the ball-milled dunite and harzburgite experiments, the precipitation of carbonate minerals began within the first few hours. The results confirmed that the newly formed $CaCO_3$ in these experiments was aragonite. The observation that the greatest amount of aragonite formed during the most milled dunite experiment suggests a positive impact of ball milling duration on the carbon sequestration efficiency through enhanced weathering of peridotites. All results indicate that ball milling can substantially enhance the weathering rate of peridotites in marine environments, promoting the immobilization of CO_2 as carbonate minerals. However, the precipitation of sepiolite could reduce the efficiency of this carbon sequestration approach over the longer term.

Acknowledgements

This work was carried out in the context of the CO2NOR Project. This project has received funding from the European Union's Horizon 2020 research and innovation programme under the Marie Sklodowska-Curie grant agreement No 654091. Additional support to Ioannis Rigopoulos was provided by the European Union FP7 Marie Curie Actions Initial Training Network CO2-

REACT (317235). For their technical assistance, we thank Philippe Besson (ICP-AES), Carole Causserand (DIC), Stéphanie Mounic (total inorganic carbon in solids), and Michel Thibaut (XRD). We thank Jacques Schott and Vasileios Mavromatis for helpful discussion.

Supplementary data

Supplementary data associated with this article can be found in the online version. These data include information about the petrographic characteristics and whole rock analyses of the starting rock materials, the composition of the artificial seawater, the saturation index values calculated using PHREEQC, details about analytical techniques, and the additional figures and tables as mentioned in the text.

References

Balaz, P., Turianicova, E., Fabian, M., Kleiv, R.A., Briancin, J., Obut, A., 2008. Structural changes in olivine $(Mg,Fe)_2SiO_4$ mechanically activated in high-energy mills. Int. J. Miner. Process. 88, 1-6.

Bonatti, E., Craig Simmons, E., Breger, D., Hamlyn, P.R., Lawrence, J., 1983. Ultramafic rock/seawater interaction in the oceanic crust: Mg-silicate (sepiolite) deposit from the Indian Ocean floor. Earth Planet. Sci. Lett. 62, 229-238.

Caldeira, K., Wickett, M.E., 2003. Anthropogenic carbon and ocean pH. Nature 425, 365.

Casey, W.H., Westrich, H.R., 1992. Control of dissolution rates of orthosilicate minerals by divalent metal–oxygen bonds. Nature 355, 157-159.

De Choudens-Sánchez, V., González, L.A., 2009. Calcite and aragonite precipitation under controlled instantaneous supersaturation: Elucidating the role of $CaCO_3$ saturation state and Mg/Ca ratio on calcium carbonate polymorphism. J. Sediment. Res. 79, 363-376.

Declercq, J., Bosc, O., Oelkers, E.H., 2013. Do organic ligands affect forsterite dissolution? Appl. Geochem. 39, 69-77.

Doney, S.C., Fabry, V.J., Feely, R.A., Kleypas, J.A., 2009. Ocean acidification: the other CO_2 problem. Ann. Rev. Marine Sci. 1, 169-192.

Dugdale, R.C., Wilkerson, F.P., 1998. Silicate regulation of new production in the equatorial Pacific upwelling. Nature 391, 270-273.

Emanuel, K., 2005. Hurricanes and global warming, Nature 436, 686-688.

514 Garcia B., Lemelle L., Rose-Koga E., Perriat P., Basset R., Gillet P. and Albarede, F., 2013. An
515 experimental model approach of biologically assisted silicate dissolution with olivine and
516 Escherichia coli - Impact on chemical weathering of mafic and atmospheric CO_2 drawdown.
517 App. Geochem. 31**,** 216-227.

518 Gerdemann, S.J., O'Connor, W.K., Dahlin, D.C., Panner, L.R., Rush, H., 2007. Ex situ aqueous
519 mineral carbonation. Environ. Sci. Technol. 41, 2587-2593.

520 Gislason, S.R., Oelkers, E.H., 2014. Carbon storage in basalt. Science 344, 373.

521 Griffioen, J., 2017. Enhanced weathering of olivine in seawater: The efficiency as revealed by
522 thermodynamic scenario analysis. Sci. Total Environ. 575, 536-544.

523 Hänchen, M., Prigiobbe, V., Storti, G., Seward, T.M., Mazotti, M., 2006. Dissolution kinetics of
524 forsteritic olivine at 90-150 ºC including effects of the presence of CO_2. Geochim.
525 Cosmochim. Acta 70, 4403-4416.

526 Hangx, S.J.T., Spiers, C.J., 2009. Coastal spreading of olivine to control atmospheric CO_2
527 concentrations: A critical analysis of viability. Int. J. Greenhouse Gas Control 3, 757-767.

528 Harrison, A.L., Power, I.M., Dipple, G.M., 2013. Accelerated carbonation of brucite in mine
529 tailings for carbon sequestration. Environ. Sci. Technol. 47, 126-134.

530 Hartmann, J., West, A.J., Renforth, P., Köhler, P., De La Rocha, C.L., Wolf-Gladrow, D.A.,
531 Dürr, H.H., Scheffran, J., 2013. Enhanced chemical weathering as a geoengineering strategy
532 to reduce atmospheric carbon dioxide, supply nutrients, and mitigate ocean acidification.
533 Rev. Geophys. 51, 113-149.

534 Hauck, J., Köhler, P., Wolf-Gladrow, D., Volker, C., 2016. Iron fertilisation and century-scale
535 effects of open ocean dissolution of olivine in a simulated CO_2 removal experiment. Environ.
536 Res. Lett. 11, 024007.

537 Haug, A.H., Kleiv, R.A., Munz, I.A., 2010. Investigating dissolution of mechanically activated
538 olivine for carbonation purposes. Appl. Geochem. 25, 1547-1563.

539 Hoegh-Guldberg, O., Mumby, P.J., Hooten, A.J., Steneck, R.S., Greenfield, P., Gomez, E.,
540 Harvell, C.D., Sale, P.F., Edwards, A.J., Caldeira, K., Knowlton, N., Eakin, C.M., Iglesias-
541 Prieto, R., Muthiga, N., Bradbury, R.H., Dubi, A., Hatziolos, M.E., 2007. Coral reefs under
542 rapid climate change and ocean acidification. Science 318, 1737-1742.

543 IPCC, 2005. In: Metz, B., Davidson, O., de Coninck, H.C., Loos, M., Meyer, L.A. (Eds.),
544 Carbon dioxide capture and storage. Cambridge University Press, Cambridge, United
545 Kingdom and New York, NY, USA, p. 442.

546 IPCC, 2007. Climate Change 2007: The Physical Science Basis. Contribution of Working Group
547 I to the Fourth Assessment Report of the Intergovernmental Panel on Climate Change.
548 Cambridge, U.K., p. 96.

549 Johnson, N.C., Burt, T., Maher, K., Rosenbauer, R.J., Bird, D., Brown, G.E., 2014. Olivine
550 dissolution and carbonation under conditions relevant for in-situ carbon storage. Chem. Geol.
551 373, 93-105.

552 Kleiv, R.A., Thornhill, M., 2006. Mechanical activation of olivine. Miner. Eng. 19, 340-347.

Köhler, P., Abrams, J.F., Völker, C., Hauck, J., Wolf-Gladrow, D.A., 2013. Geoengineering impact of open ocean dissolution of olivine on atmospheric CO_2, surface ocean pH and marine biology. Environ. Res. Lett. 8, art. no. 014009.

Köhler, P., Hartmann, J., Wolf-Gladrow, D.A., 2010. Geoengineering potential of artificially enhanced silicate weathering of olivine. PNAS 107, 20228-20233.

Lackner, K.S., 2003. A guide to CO_2 sequestration. Science 300, 1677-1678.

Lackner, K.S., Wendt, C.H., Butt, D.P., Joyce, E.L., Sharp, D.H., 1995. Carbon dioxide disposal in carbonate minerals. Energy 20, 1153-1170.

Li, J., Hitch, M., 2016a. Characterization of the microstructure of mechanically-activated olivine using X-ray diffraction pattern analysis. Miner. Eng. 86, 24-33.

Li, J., Hitch, M., 2016b. Mechanical activation of ultramafic mine waste rock in dry condition for enhanced mineral carbonation. Miner. Eng. 95, 1-4.

Li, J., Hitch, M., 2017a. Ultra-fine grinding and mechanical activation of mine waste rock using a planetary mill for mineral carbonation. Int. J. Miner. Process. 158, 18-26.

Li, J., Hitch, M., 2017b. Structural and chemical changes in mine waste mechanically-activated in various milling environments. Powder Technol. 308, 13-19.

Marion, G.M., Millero, F.J., Camoes, M.F., Spitzer, P., Feistel, R., Chen, C.-T.A., 2011. pH of seawater. Mar. Chem. 126, 89-96.

Matter, J.M., Kelemen, P.B., 2009. Permanent storage of carbon dioxide in geological reservoirs by mineral carbonation. Nature Geosci. 2, 837-841.

Matter, J.M., Stute, M., Snæbjörnsdottir, S.Ó., Oelkers, E.H., Gislason, S.R., Aradottir, E.S., Sigfusson, B., Gunnarsson, I., Sigurdardottir, H., Gunnlaugsson, E., Axelsson, G., Alfredsson, H.A., Wolff-Boenisch, D., Mesfin, K., de la Reguera Taya, D.F.; Hall, J., Dideriksen, K., Broecker, W.S., 2016. Rapid carbon mineralization for permanent disposal of anthropogenic carbon dioxide emissions. Science 352, 1312-1314.

Meysman, F.J.R., Montserrat, F., 2017. Negative CO_2 emissions via enhanced silicate weathering in coastal environments. Biol. Lett. 13: 20160905.

Michael, K., Golab, A., Shulakova, V., Ennis-King, J., Allinson, G., Sharma, S., Aiken, T., 2010. Geological storage of CO_2 in saline aquifers - A review of the experience from existing storage operations. Int. J. Greenhouse Gas Control 4, 659-667.

Millero, F.J., Graham, T.B., Huang, F., Bustos-Serrano, H., Pierrot, D., 2006. Dissociation constants of carbonic acid in seawater as a function of salinity and temperature. Mar. Chem. 100, 80-94.

Montserrat, F., Renforth, P., Hartmann, J., Leermakers, M., Knops, P., Meysman, F.J.R., 2017. Olivine dissolution in seawater: Implications for CO_2 sequestration through enhanced weathering in coastal environments. Environ. Sci. Technol. 51, 3960-3972.

Moosdorf, N., Renforth, P., Hartmann, J., 2014. Carbon dioxide efficiency of terrestrial enhanced weathering. Environ. Sci. Technol. 48, 4809-4816.

Morse, J.W., Arvidson, R.S., Lüttge, A., 2007. Calcium carbonate formation and dissolution. Chem. Rev. 107, 342-381.

Morse, J.W., Wang, Q., Tsio, M.Y., 1997. Influences of temperature and Mg:Ca ratio on $CaCO_3$ precipitates from seawater. Geology 25, 85-87.

Mukasa, S.B., Ludden, J.N., 1987. Uranium–lead ages of plagiogranites from the Troodos ophiolite, Cyprus, and their tectonic significance. Geology 15, 825-828.

Munz, I.A., Brandvoll, Ø., Haug, T.A., Iden, K., Smeets, R., Kihle, J., Johansen, H., 2012. Mechanisms and rates of plagioclase carbonation reactions. Geochim. Cosmochim. Acta 77, 27-51.

Oelkers, E.H., 2001. An experimental study of forsterite dissolution rate as a function of temperature and aqueous Mg and Si concentration. Chem. Geol. 148, 485-494.

Oelkers, E.H., Benning, L.G., Lutz, S., Mavromatis, V., Pearce, C.R., Plümper, O., 2015. The efficient long-term inhibition of forsterite dissolution by common soil bacteria and fungi at Earth surface conditions. Geochim. Cosmochim. Acta 168, 222-235.

Oelkers, E.H., Cole, D.R., 2008. Carbon Dioxide Sequestration. A solution to a global problem. Elements 4, 305-310.

Oelkers, E.H., Gislason, S.R., Matter, J., 2008. Mineral carbonation of CO_2. Elements 4, 333-337.

Okland, I., Huang, S., Thorseth, I.H., Pedersen, R.B., 2014. Formation of H_2, CH_4 and N-species during low-temperature experimental alteration of ultramafic rocks. Chem. Geol. 387, 22-34.

Orr, J.C., Fabry, V.J., Aumont, O., Bopp, L., Doney, S.C., Feely, R.A., Gnanadesikan, A., Gruber, N., Ishida, A., Joos, F., Key, R.M., Lindsay, K., Maier-Reimer, E., Matear, R., Monfray, P., Mouchet, A., Najjar, R.G., Plattner, G.-K., Rodgers, K.B., Sabine, C.L., Sarmiento, J.L., Schlitzer, R., Slater, R.D., Totterdell, I.J., Weirig, M.-F., Yamanaka, Y., Yool, A., 2005. Anthropogenic ocean acidification over the twenty-first century and its impact on calcifying organisms. Nature 437, 681-686.

Parkhurst, D.L., Appelo, C.A.J., 2013. Description of Input and Examples for PHREEQC Version 3–A Computer Program for Speciation, Batch-Reaction, One-Dimensional Transport, and Inverse Geochemical Calculations; U.S. Geological Survey Techniques and Methods: Denver, CO, Vol. book 6, p. 497.

Pokrovsky, O.S., Schott, J., 2000. Kinetics and mechanism of forsterite dissolution at 25 ºC and pH from 1 to 12. Geochim. Cosmochim. Acta 64, 3313-3325.

Power, I.M., Harrison, A.L., Dipple, G.M., Wilson, S.A., Kelemen, P.B., Hitch, M., Southam, G., 2013. Carbon mineralization: from natural analogues to engineered systems. Rev. Mineral. Geochem. 77, 305-360.

Power, I.M., Harrison, A.L., Dipple, G.M., 2016. Accelerating mineral carbonation using carbonic anhydrase. Environ. Sci. Technol. 50, 2610-2618.

Radziszewski, P., 2013. Energy recovery potential in comminution processes. Miner. Eng. 46-47, 83-88.

Ragueneau, O., Schultes, S., Bidle, K., Claquin, P., Moriceau, B., 2006. Si and C interactions in the world ocean: importance of ecological processes and implications for the role of diatoms in the biological pump. Glob. Biogeochem. Cycles 20, GB4S02.

633 Renforth, P., 2012. The potential of enhanced weathering in the UK. Int. J. Greenhouse Gas
634 Control 10, 229-243.

635 Renforth, P., Henderson, G., 2017. Assessing ocean alkalinity for carbon sequestration. Rev.
636 Geophys., 55, doi:10.1002/2016RG000533.

637 Ricke, K.L., Orr, J.C., Schneider, K., Caldeira, K., 2013. Risks to coral reefs from ocean
638 carbonate chemistry changes in recent earth system model projections. Environ. Res. Lett. 8,
639 034003.

640 Rignot, E.J., 1998. Fast recession of a West Antarctic glacier. Science 281, 549-551.

641 Rigopoulos, I., Tsikouras, B., Pomonis, P., Hatzipanagiotou, K., 2013. Petrographic investigation
642 of microcrack initiation in mafic ophiolitic rocks under uniaxial compression. Rock Mech.
643 Rock Eng. 46 (5), 1061-1072.

644 Rigopoulos, I., Petallidou, K.C., Vasiliades, M.A., Delimitis, A., Ioannou, I., Efstathiou, A.M.,
645 Kyratsi, Th., 2015. Carbon dioxide storage in olivine basalts: effect of ball milling process.
646 Powder Technol. 273, 220-229.

647 Rigopoulos, I., Vasiliades, M.A., Ioannou, I., Efstathiou, A.M., Godelitsas, A., Kyratsi, Th.,
648 2016a. Enhancing the rate of ex situ mineral carbonation in dunites. Adv. Powder Technol.
649 27, 360-371.

650 Rigopoulos, I., Petallidou, K.C., Vasiliades, M.A., Delimitis, A., Ioannou, I., Efstathiou, A.M.,
651 Kyratsi, Th., 2016b. On the potential use of quarry waste material for CO_2 sequestration. J.
652 CO_2 Util. 16, 361-370.

653 Robertson, A.H.F., 2002. Overview of the genesis and emplacement of Mesozoic ophiolites in
654 the Eastern Mediterranean Tethyan region. Lithos 65, 1-67.

655 Robinson, P.T., Malpas, J., 1990. The Troodos Ophiolite of Cyprus: new perspectives on its
656 origin and emplacement. In *Ophiolites: Oceanic Crustal Analogues*; Malpas, J., Moores, E.
657 M., Panayiotou, A., Xenophontos, C., Eds.; Cyprus Geol. Surv. Dept., Nicosia, pp. 13-36.

658 Saldi, G.D., Jordan, G., Schott, J., Oelkers, E.H., 2009. Magnesite growth rates as a function of
659 temperature and saturation state. Geochim. Cosmochim. Acta 73, 5646-5657.

660 Schiermeier, Q., 2011. Increased flood risk linked to global warming, Nature 470, 316.

661 Schuiling, R.D., De Boer, P.L., 2011. Rolling stones; fast weathering of olivine in shallow seas
662 for cost-effective CO_2 capture and mitigation of global warming and ocean acidification.
663 Earth Syst. Dynam. Discuss. 2, 551-568.

664 Schuiling, R.D., Krijgsman, P., 2006. Enhanced weathering: an effective and cheap tool to
665 sequester CO_2. Clim. Chang. 74, 349-354.

666 Seifritz, W., 1990. CO_2 disposal by means of silicates. Nature 345, 486.

667 Shirokava, L.S., Benezeth, P., Pokrovsky, O.S. Gerard, E., Menez, B., Alfredsson, H., 2012.
668 Effect of the heterotrophic bacterium Psuedomonas reactans on olivine dissolution kinetics
669 and implications for CO_2 storage in basalts. Geochim. Cosmochim. Acta 80, 30-50.

670 Solomon, S., Plattner, G.K., Knutti, R., Friedlingstein, P., 2009. Irreversible climate change due
671 to carbon dioxide emissions. PNAS 106, 1704-1709.

672 Stockmann G.J., Wolff-Boenisch D., Bovet, N., Gislason S.R. and Oelkers E.H., 2014. The role
673 of silicate surfaces on calcite precipitation kinetics. Geochim. Cosmochim. Acta. 135, 231-
674 250.

675 Sun, W., Jayaraman, S., Chen, W., Persson, K.A., Ceder, G., 2015. Nucleation of metastable
676 aragonite $CaCO_3$ in seawater. PNAS 112 (11), 3199-3204.

677 Taylor, L.L., Quirk, J., Thorley, R.M.S., Kharecha, P.A., Hansen, J., Ridgwell, A., Lomas, M.R.,
678 Banwart, S.A., Beerling, D.J., 2016. Enhanced weathering strategies for stabilizing climate
679 and averting ocean acidification. Nat. Clim. Change 6, 402-408.

680 Tollefson, J., 2008. UN decision puts brakes on ocean fertilization. Nature 453, 704.

681 Trenberth, K.E., Dai, A., Van Der Schrier, G., Jones, P.D., Barichivich, J., Briffa, K.R.,
682 Sheffield, J., 2014. Global warming and changes in drought. Nature Clim. Change 4, 17-22.

683 Turianicová, E., Baláž, P., Tuček, L., Zorkovská, A., Zeleňák, V., Németh, Z., Šatka, A., Kováč,
684 J., 2013. A comparison of the reactivity of activated and non-activated olivine with CO_2. Int.
685 J. Miner. Process. 123, 73-77.

686 van Haren, J., Dontsova, K., Barron-Gafford, G.A., Troch, P.A., Chorover, J., Delong, S.B.,
687 Breshears, D.D., Huxman, T.E., Pelleties, J.D., Saleska, S.R., Xeng, X., Ruiz, J., 2017. CO_2
688 diffusion into pore spaces limits weathering rate of an experimental basalt landscape.
689 Geology, DOI: 10.1130/G38569.1.

690 Wang, F., Giammar, D.E., 2013. Forsterite dissolution in saline water at elevated temperature
691 and high CO_2 pressure. Environ. Sci. Technol. 47, 168-173.

692 Wilson, S.A., Barker, S.L.L., Dipple, G.M., Atudorei, V., 2010. Isotopic disequilibrium during
693 uptake of atmospheric CO_2 into mine process waters: implications for CO_2 sequestration.
694 Environ. Sci. Technol. 44, 9522-9529.

695 Wilson, S.A., Harrison, A.L., Dipple, G.M., Power, I.M., Barker, S.L.L., Ulrich Mayer, K.,
696 Fallon, S.J., Raudsepp, M., Southam, G., 2014. Offsetting of CO_2 emissions by air capture in
697 mine tailings at the Mount Keith Nickel Mine, Western Australia: Rates, controls and
698 prospects for carbon neutral mining. Int. J. Greenhouse Gas Control 25, 121-140.

699 Wolff-Boenisch, D., Wenau, S., Gislason, S.R., Oelkers, E.H., 2011. Dissolution of basalts and
700 peridotite in seawater, in the presence of ligands, and CO_2: Implications for mineral
701 sequestration of carbon dioxide. Geochim. Cosmochim. Acta 75, 5510-5525.

702

703

704

705

706

707

FIGURE CAPTIONS

Fig. 1. BET (m^2 g^{-1}) specific surface area versus ball milling time for the studied rock materials (red circles show the milled samples used during the experiments). The BET values for the milled basalt and dunite samples were acquired from Rigopoulos et al. (2015) and Rigopoulos et al. (2016a), respectively.

Fig. 2. Experimental design used for the enhanced weathering experiments.

Fig. 3. Temporal evolution of the reactive fluid pH: (a) Control experiment, and experiments with unmilled and milled dunite; (b) Control experiment, and experiments with unmilled and milled basalt and harzburgite.

Fig. 4. Temporal evolution of the reactive fluid dissolved inorganic carbon (DIC) concentration: (a) Control experiment, and experiments with unmilled and milled dunite; (b) Control experiment and experiments with unmilled and milled basalt and harzburgite.

731 **Fig. 5.** Temporal evolution of the reactive fluid Si (a), Mg (b), and Ca (c) concentrations in all
732 experiments.
733
734 **Fig. 6.** Temporal evolution of the aragonite, calcite and sepiolite saturation indices, for the
735 experiments with the milled (a-f) dunite, and (g-i) harzburgite. Saturation indices were
736 determined using PHREEQC V3 and its llnl database (Parkhurst and Appelo, 2013).
737
738 **Fig. 7.** SEM images showing the significant reduction of particle size after ball milling: (a)
739 unmilled (SM15), and (b) milled (BM46) dunite; (c) unmilled (SM17), and (d) milled (BM72)
740 harzburgite; (e) unmilled (SM1), and (f) milled (BM7) basalt. The unmilled rock samples were
741 cleaned ultrasonically in ethanol, thus they are free of fine particles. The magnification in (a,c,e)
742 is significantly lower compared to (b,d,f).
743
744 **Fig. 8.** Temporal evolution of solid $CaCO_3$ content for the experiments with the milled (a,b)
745 dunite, and (c) harzburgite.
746
747 **Fig. 9.** Transmission electron microscopy images (clockwise from top left) of the most milled
748 dunite (sample BM46) after the experiment, depicting: (a,b) the precipitated aragonite. Moiré
749 fringes, such as these pointed by black arrow in (a) were usually observed and prove that
750 aragonite crystals are highly crystalline. White arrows in (b) denote aragonite nanocrystals (also
751 circled); (c) the structural disordering of olivine, due to the amorphous-like contrast of the
752 nanoparticle, and (d) the precipitated sepiolite (the black arrows show the crystal boundaries).

753 The SAD pattern inset confirms both its chemical composition [$Mg_4Si_6O_{15}(OH)_2 \cdot 6H_2O$] and its
754 low crystallinity.

Table 1
Ball milling conditions and specific surface area values of the unmilled and milled rock materials (data for the milled samples of basalt and dunite acquired from Rigopoulos et al. (2015a) and Rigopoulos et al. (2016a), respectively).

Sample code	Ball milling conditions		BET (m^2 g^{-1}) Specific surface area
	Milling time (h)	Type of milling	
SM15 (Unmilled Dunite)	-	-	0.4
BM38 (Milled Dunite)	4	Wet (50 wt% Ethanol)	35.7
BM46 (Milled Dunite)	20	Wet (50 wt% Ethanol)	64.6
SM17 (Unmilled Harzburgite)	-	-	0.5
BM72 (Milled Harzburgite)	16	Wet (50 wt% Ethanol)	53.1
SM1 (Unmilled Basalt)	-	-	2.0
BM7 (Milled Basalt)	4	Wet (50 wt% Ethanol)	58.9

Table 2
Calculations of $CaCO_3$ abundance in the studied rock materials based on (i) the content of total inorganic carbon in the solid phase (the sequestration efficiency of each rock material during the 2-month experiments is also given), and (ii) mass balance from the fluid phase assuming no change in total solids mass due to dissolution.

Sample code/rock material	$CaCO_3$ wt% based on the measured total inorganic carbon in solids			Sequestration efficiency (g CO_2/ g rock)	$CaCO_3$ wt% calculated at the end of the experiment based on mass balance from the fluid phase
	Before the experiment	After the experiment	$CaCO_3$ formed during the experiment		
SM15/Unmilled Dunite	0.1	0.7	0.6	0.003	2.1
BM38/Milled Dunite	0.8	7.4	6.6	0.029	10.7
BM46/Milled Dunite	1.2	11.2	10	0.044	16.6
SM17/Unmilled Harzburgite	0.3	0.6	0.3	0.001	1.6
BM72/Milled Harzburgite	0.9	7.6	6.7	0.029	10.6
SM1/Unmilled Basalt	0.4	0.4	0	0.000	0
BM7/Milled Basalt	0.6	2.1	1.5	0.007	0

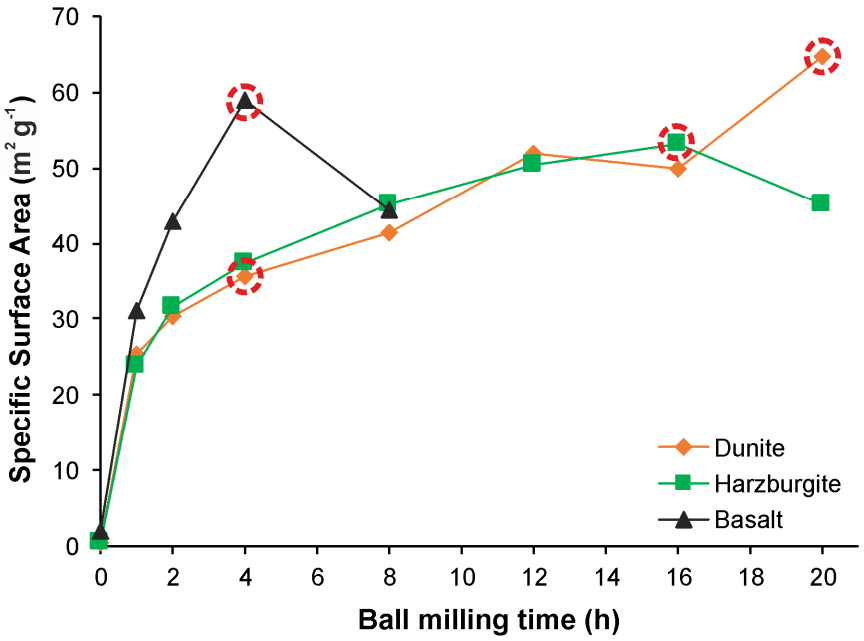

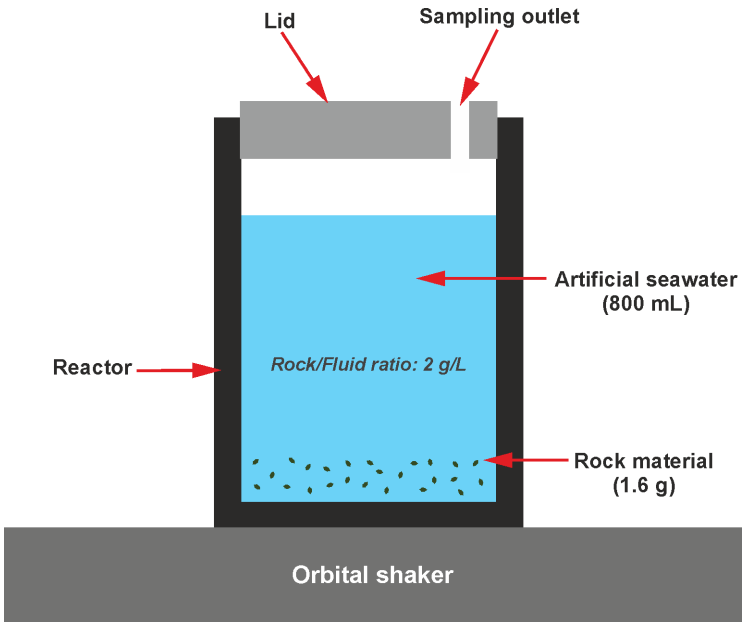

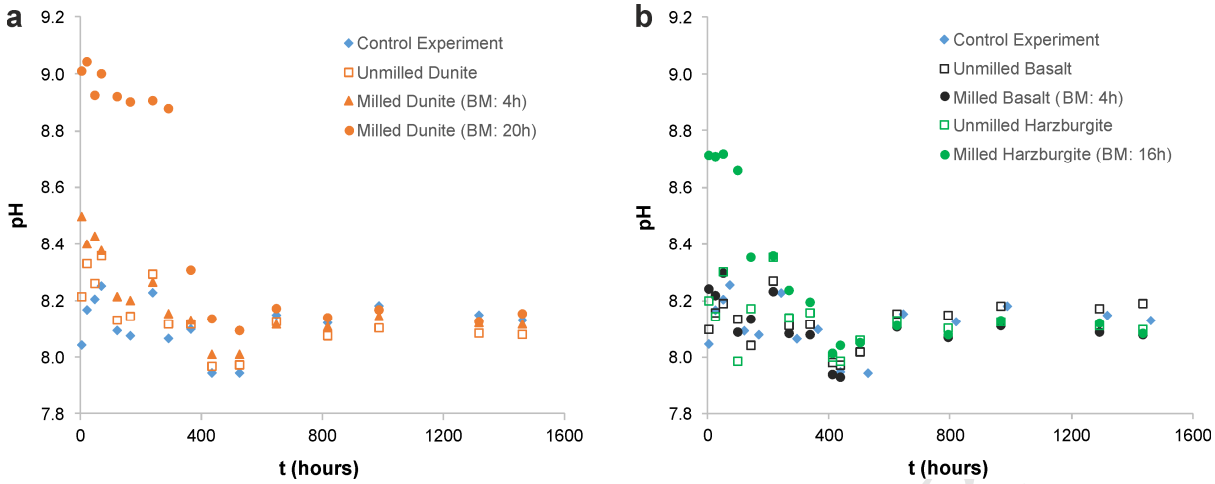

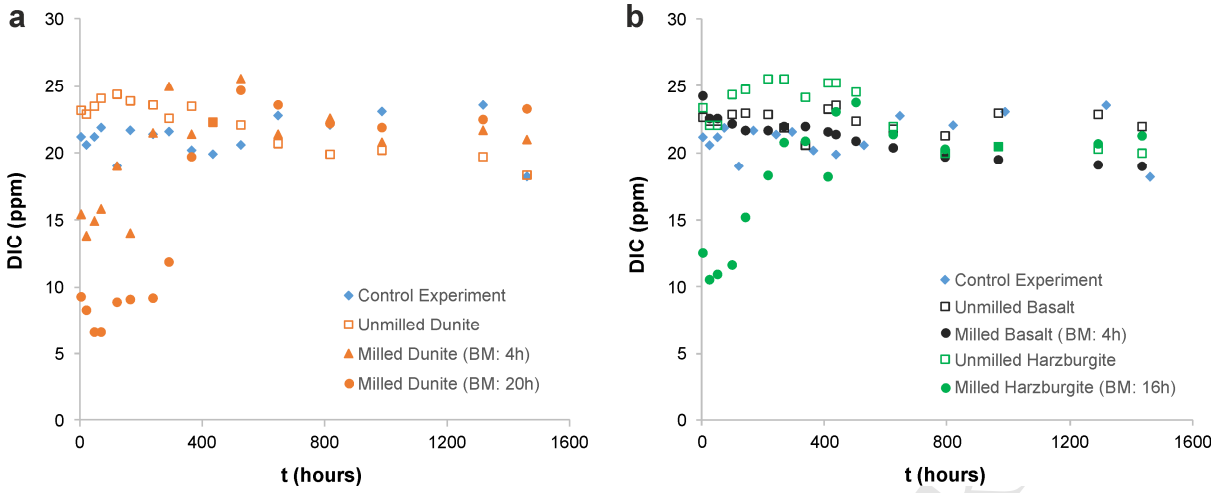

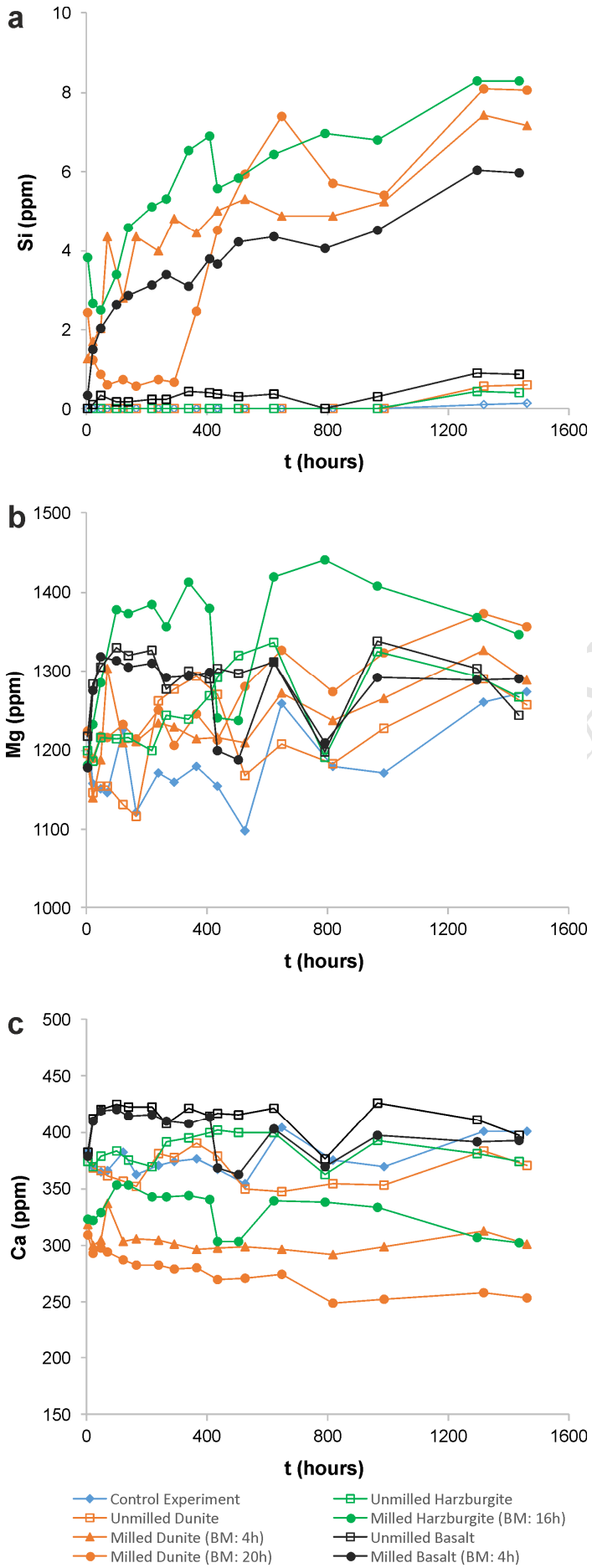
a
Si (ppm)
t (hours)
b
Mg (ppm)
t (hours)
c
Ca (ppm)
t (hours)
Control Experiment
Unmilled Dunite
Milled Dunite (BM: 4h)
Milled Dunite (BM: 20h)
Unmilled Harzburgite
Milled Harzburgite (BM: 16h)
Unmilled Basalt
Milled Basalt (BM: 4h)

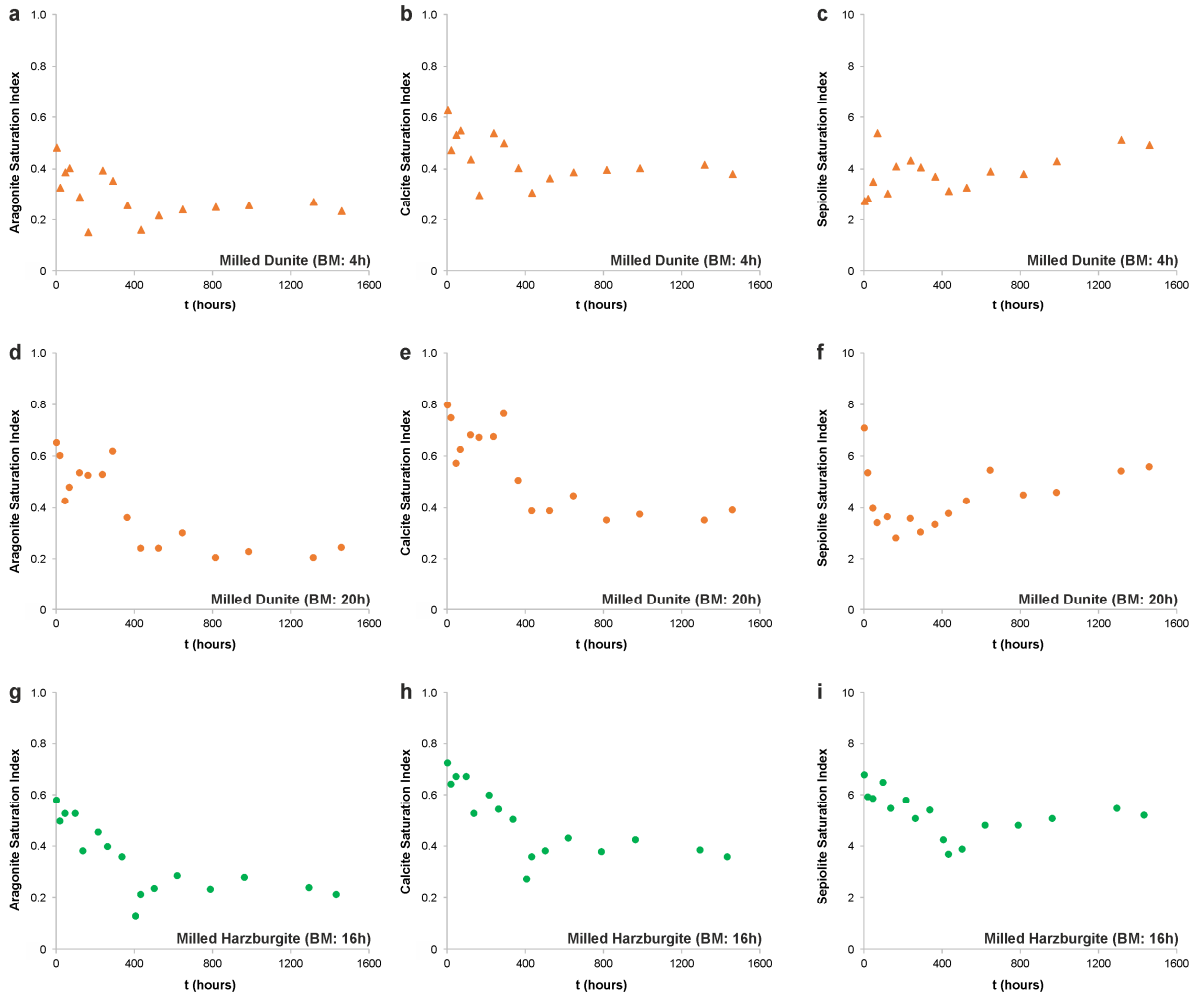

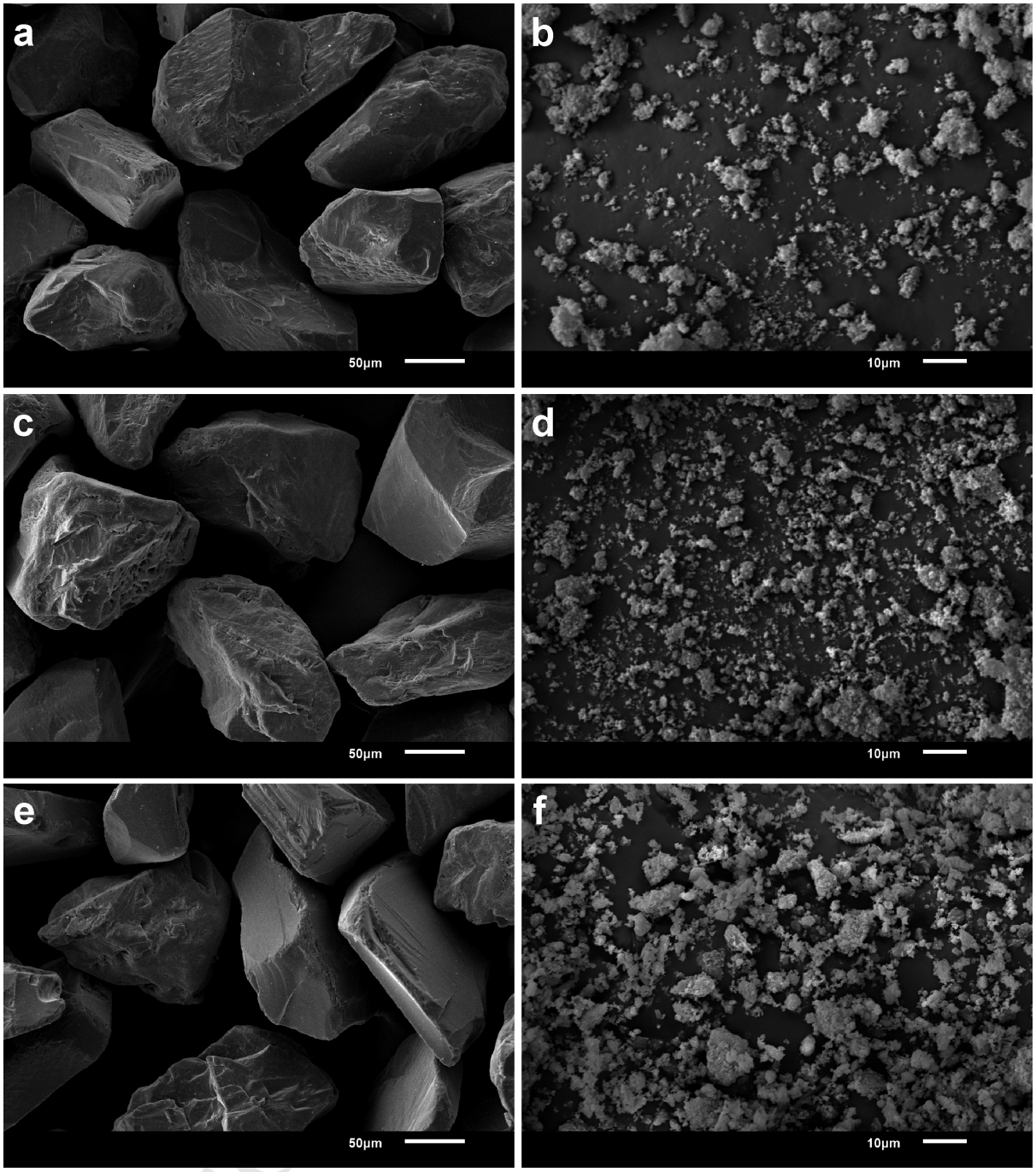
a
50µm
b
10µm
c
50µm
d
10µm
e
50µm
f
10µm

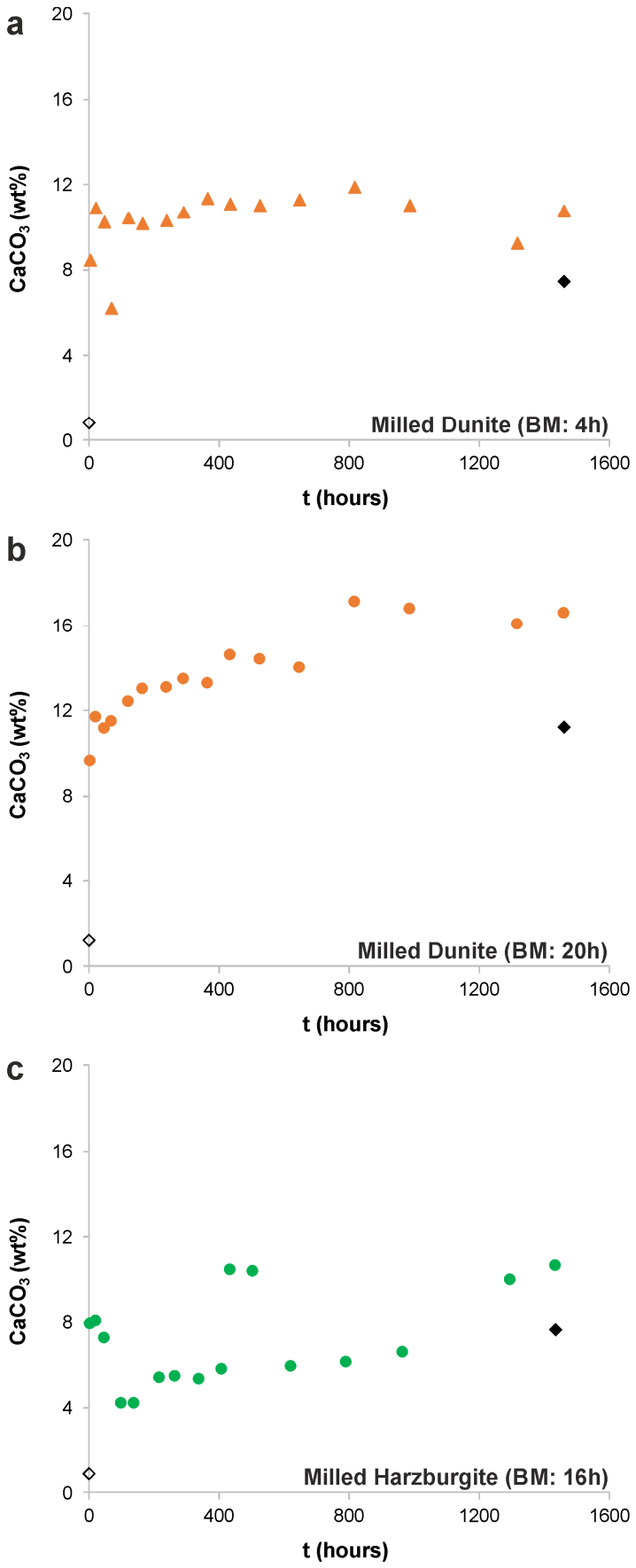
a
b
c
CaCO3 (wt%)
t (hours)
Milled Dunite (BM: 4h)
Milled Dunite (BM: 20h)
Milled Harzburgite (BM: 16h)
0
4
8
12
16
20
0
400
800
1200
1600
Based on mass balance from the fluid phase
Based on the total inorganic carbon in the solid before the experiment
Based on the total inorganic carbon in the solid after the experiment

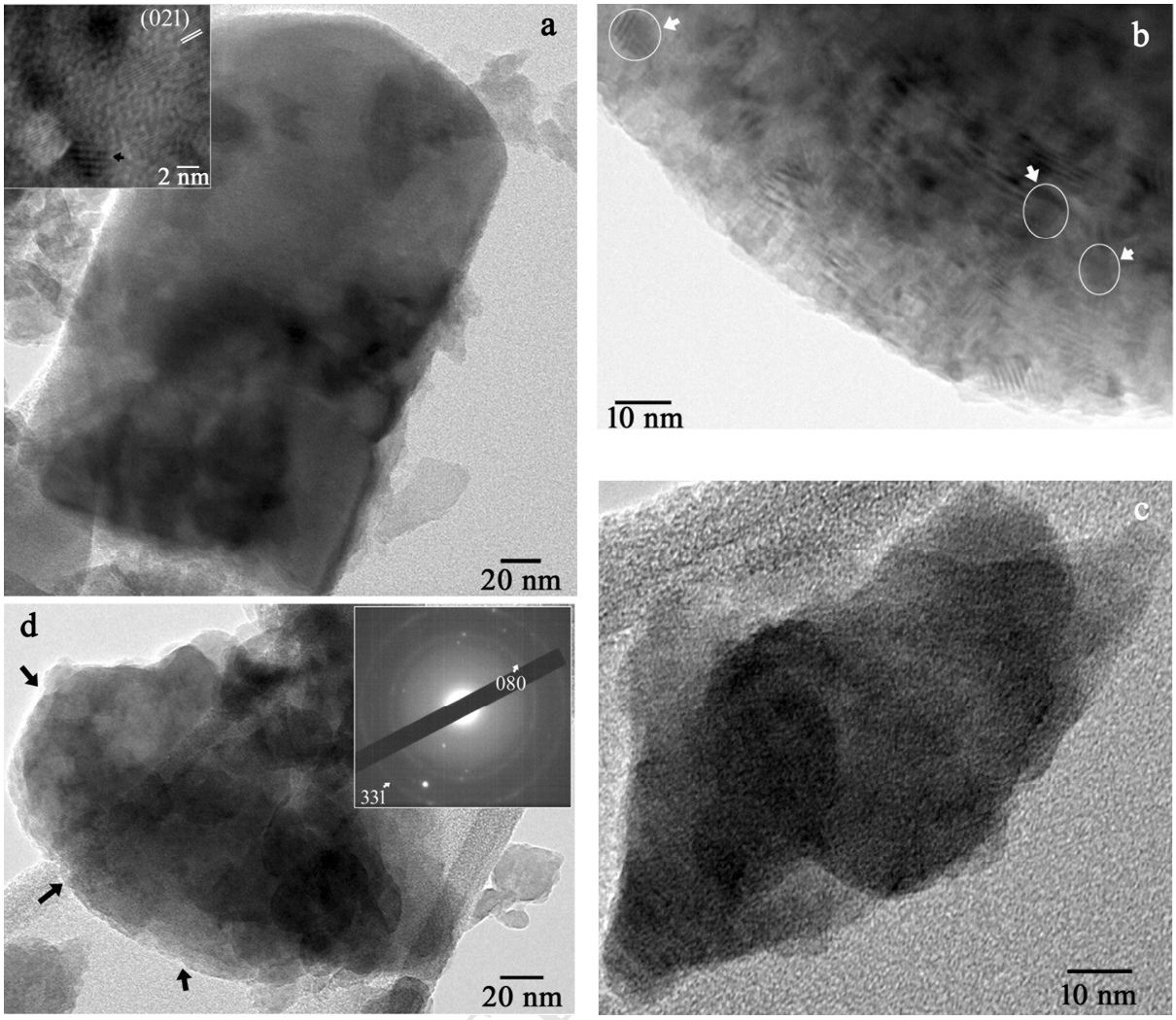

Highlights

- Enhanced weathering of ultrafine peridotites and basalts in seawater was studied.
- Open system experiments were performed in batch reactors at ambient conditions.
- Peridotites induced CO_2 drawdown directly from the atmosphere via mineralization.
- The basalt did not yield any significant changes in seawater composition.
- The precipitation of sepiolite could reduce the carbon sequestration efficiency.